Characterization of the Miscibility of Poly(butyl methacrylate) with a Nonylphenol Ethoxylate Surfactant and with Various Poly(ethylene glycol) Oligomers

Ewa Odrobina, Jianrong Feng,† Seigou Kawaguchi,‡ and Mitchell A. Winnik*

Department Of Chemistry, University of Toronto, 80 St. George Street, Toronto, ON, Canada M5S 3H6

Michael Neag and Edwin F. Meyer

ICI Paints, 16651 Sprague Road, Strongsville Ohio 44138

Received December 29, 1997; Revised Manuscript Received July 16, 1998

ABSTRACT: Previous experiments from the Winnik group (e.g., *Macromol. Rapid Commun.* **1995**, *16*, 861) have established that several nonylphenol ethoxylate surfactants were miscible with poly(butyl methacrylate) (PBMA) latex films at 90 °C, and act as plasticizers to accelerate polymer diffusion rates in the films. Here we turn our attention to the question of miscibility at room temperature. Using modulated DSC, we show that a nonylphenol ethoxylate (NP-20, with 20 ethylene oxide units, EO_{20}) has only limited (ca. 2 wt %) miscibility with high molecular weight PBMA latex films at room temperatures and that corresponding poly(ethylene glycol) (PEG) oligomers EO_x ($x = 10, 20$) have even lower miscibility. Miscibility is detected as a decrease in the glass transition temperature of the polymer; and immiscibility, as a melting endotherm of the surfactant component. In addition, we examine the influence of the EO_x oligomers on the polymer diffusion rate in PBMA latex films. Oligomers larger than EO_{10} retard the rate of interparticle polymer diffusion.

Introduction

Surfactants play an important role in latex film formation, and their presence has a strong influence on the final properties of the latex film. The presence of surfactant in the film can affect various properties of the film, including its glass transition,[1,2] its dynamic mechanical properties,[3] its peel strength,[4] and its water resistance.[5] The magnitude of these effects depend sensitively on the location of the surfactant in the film. If miscible with the latex polymer, the surfactant can dissolve in the film resin.[6−8] If miscibility is low, the excess surfactant can form occlusions in the film or migrate to the air or substrate surfaces.[9−11] We are interested in understanding how the chemical structure of surfactants influences the latex film formation process. In previous experiments, we have examined how the presence of surfactants affects the rate of water evaporation[12] as the film dries, the packing structure of the latex particles,[13,14] and the coalescence and polymer interdiffusion processes.[6,9,11]

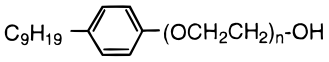

n = 20 NP-20

When the surfactant can dissolve in the latex polymer, it can act as a plasticizer. Kawaguchi et al.[6] examined the effect of a nonylphenol ethoxylate (NP-20, with 20 ethylene oxide units, EO_{20}) on polymer interdiffusion rates in PBMA latex films at 90 °C. Using a fluorescence energy transfer method (see below), they measured the influence of this surfactant on the rate of mixing of polymers in adjacent cells in latex films. They observed that small amounts (3 wt %) of NP-20 in the dry film accelerated the polymer diffusion rate significantly, and increasing the amount of surfactant to 15 wt % led to a 2-order-of-magnitude increase in the diffusion rate. They calculated apparent diffusion coefficients (D_{app}) from their data and showed that the influence of NP-20 on D_{app} could be analyzed quantitatively in terms of the Fujita−Doolittle free volume model, as shown in Figure 1. In this model, the diffusion coefficient increases with the volume fraction

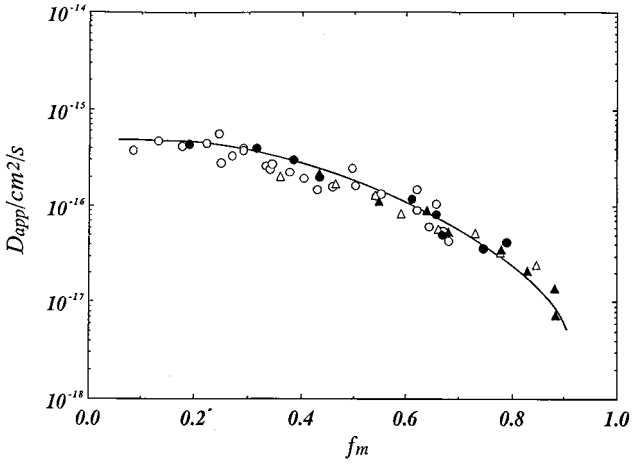

Figure 1. Master curve of apparent diffusion coefficient (D_{app}) values vs extent of mixing (f_m) for PBMA films in the presence of different amounts NP-20. The data are taken from ref 6a. Added amounts of NP-20 up to 15 wt % increased the diffusion rate of PBMA by up to 2 orders of magnitude for films annealed at 90 °C. The master curve was generated[6a] by fitting the D_{app} values to the Fujita−Doolittle free volume model.[6b]

* To whom correspondence should be addressed: e-mail mwinnik@chem.utoronto.ca.

† Permanent address: The Thompson−Gordon Group, 3225 Mainway, Burlington, ON L7M 1A6, Canada.

‡ Permanent address: Department of Materials Science, Toyohashi University of Technology, Tempaku-cho, Toyohashi 441, Japan.

10.1021/ma971870c CCC: $15.00
Published on Web 09/24/1998

Table 1. Recipe for the Preparation of Labeled PBMA Latex

first stage		second stage	
BMA (mL)	3.3	BMA (mL)	30
water (mL)	60	AnMA[c](g)	0.910
KPS[a](g)	0.066	water (mL)	24
SDS[b](g)	0.1	KPS (g)	0.06
$NaHCO_3$ (g)	0.066	SDS (g)	0.54
temp (°C)	80	temp (°C)	80
time (h)	1	time (h)	4

[a] KPS: potassium persulfate. [b] SDS: sodium dodecyl sulfate. [c] AnMA: 9-anthryl methacrylate. For phenanthrene-labeled latex, 0.576 g of PheMMa [(9-phenanthryl)methyl methacrylate] dye comonomer was used.

Table 2. Latex Particle Characteristics

Phe-PBMA	An-PBMA
High *M* latex:	
$M_n = 120$ K	$M_n = 133$ K
$M_w = 38$ K	$M_w = 42$ K
$M_w/M_n = 2.9$	$M_w/M_n = 3.16$
$d = 124$ nm (0.040)[a]	$d = 132$ nm (0.037)[a]
Low *M* latex:	
$M_w = 33\,900$	$M_w = 35\,700$
$M_n = 18\,300$	$M_n = 16\,700$
$M_w/M_n = 1.85$	$M_w/M_n = 2.14$
$d = 119$ nm (0.03)[a]	$d = 119$ nm (0.035)[a]

[a] Size polydispersity.

ϕ_a of additive, and all the data can be shifted to generate a master curve with a single fitting parameter that describes the difference in free volume between the polymer and the plasticizer additive.

From these results we deduced that the surfactant and polymer were miscible at 90 °C for the range of compositions examined. Other questions remain. For example, what happens at room temperature? When does the surfactant enter the polymer phase? What drives the miscibility, the PEG chain, or the NP-hydrophobic group? To address some of these questions, we have extended our interdiffusion studies to examine the effect of PEG oligomers on the PBMA diffusion rate, and we have carried out modulated differential scanning calorimetry (DSC) measurements on PBMA latex films, in the presence and absence of these additives. In modulated DSC (MDSC), a sinusoidal oscillation in temperature is superimposed on the normal temperature ramp, in both the heating and cooling cycles. In this way, one can separate the reversible and irreversible components of a thermal transition and obtain a more precise measurement of the glass transition temperature (T_g) of the film. One of the signatures of miscibility of a plasticizer in a polymer is a lowering of the polymer T_g. The additives examined by MDSC were NP-20 and two PEG oligomers, EO_{10} and EO_{20}.

Experimental Section

Materials. Unlabeled poly(butyl methacrylate) (PBMA) aqueous latex particles with diameters of 144 nm were prepared at 30 wt % solids by conventional emulsion polymerization using a procedure similar to that reported previously.[15] By gel permeation chromatography (GPC, poly(methyl methacrylate) standards) the PBMA had $M_w = 3.85 \times 10^5$ with $M_w/M_n = 2.67$. This material was employed in the MDSC experiments. Polymer diffusion experiments were carried out on labeled PBMA samples, of both high molecular weight ($M_w = 4 \times 10^5$) and low molecular weight ($M_w = 3.5 \times 10^4$) (PBMA). Both sets of polymers had $M_w/M_n = 2.5-3$ and a degree of labeling of 0.8 mol %. Film samples were prepared from a 1:1 mixture of donor- (phenanthrene) and acceptor-labeled (anthracene) polymer, referred to as Phe-PBMA and An-PBMA, respectively, matched as closely as possible in molecular weight, molecular weight distribution, and particle size. To help control these features of the reaction, both the donor- and acceptor-labeled latex were prepared from a common unlabeled seed, and both emulsion polymerization reactions were run under strictly identical conditions. The recipes employed in the syntheses of the latex dispersions and the characteristics of the latex particles are presented in Tables 1 and 2.

Surfactant (sodium dodecyl sulfate) and low molecular weight salts used in the preparation of the latex dispersions, were completely removed by ion exchange (Bio-Rad, AG-501-X8 mixed bed resin, 3 g resin per 100 mL of latex). The procedure was repeated three times. (Nonylphenoxy)poly(ethylene oxide) NP-20 (TCI) and poly(ethylene glycol) (PEG-*n*, EO_n); $n = 10$, 20, 45, 68, 100 (Aldrich) were used without further purification. The synthesis of the donor- and acceptor-labeled PBMA latex particles was described previously.[16,17]

NP-20 Binding Isotherms. PBMA latex particles with diameters of 393, 261, 141 nm were used for binding isotherm measurements. These latex dispersions were prepared in a way similar to that reported previously.[15] The binding isotherms were obtained by equilibrating known amounts of latex and surfactant, centrifuging the dispersion to sediment the latex, and measuring the concentration of surfactant in supernatant (c_s) by UV−Vis spectroscopy. The measurements were made at the NP-20 absorption peak at $\lambda = 276$ nm with extinction coefficient $\epsilon = 1347$ M^{-1} cm^{-1}. Different amounts of a stock solution (5.0544×10^{-3} M NP-20) were added to aliquots of a latex dispersion. Next the samples where shaken for a few hours and left overnight to equilibrate. The samples were then centrifuged at 10 000 and 14 000 rpm, respectively, for 10 min with an Eppendorf 5415C centrifuge for the 393 and 261 nm PBMA latex particles. For the latex with a diameter of 141 nm, a Beckman Instruments L550 B ultracentrifuge was used at 30 000 rpm. The centrifugation time was 20 min. In the case of the 393 and 261 nm PBMA latex, after centrifugation, the supernatant was filtered through a 0.2 μm single-use filter from Gelman Sciences (product no. 4454). Finally, the number of NP-20 molecules per latex (Γ, the surface concentration) was calculated using the following equation: $(\Gamma = (c_i - c_s)V/S$, where c_i is the initial concentration of NP-20 in the latex dispersion, c_s is the concentration of the surfactant in supernatant calculated from UV absorption measurements, V is the volume of sample (0.2 mL), and S is the total surface area (number of particles times the surface area per particle). A plot of Γ vs c_s yields the binding isotherm curves for NP-20. The plateau of the curve gives us the saturation value of Γ, (Γ_{sat}), from which we calculate the mean area per surfactant of the NP−$(EO)_x$ molecules at saturation.

Sample Preparation. NP-20 surfactant was added to the PBMA latex dispersions to obtain samples with 2, 5, or 10 wt % of surfactant based upon latex solids. The mixtures were gently shaken for a few hours and left overnight to equilibrate. Then the dispersions were cast onto glass plates, each covered with an inverted Petri dish, and placed in an oven at 32 °C to form dry and transparent films. Because the wet films are covered in this way during drying, water evaporation is slow (e.g., 4 h), and most of the drying occurs at 100% relative humidity. Films containing EO_{10} and EO_{20} were prepared in the same manner. In some experiments with NP-20 surfactant, films were prepared through more rapid drying at 65% relative humidity. In this case the samples were simply not covered with a Petri dish (drying time, e.g., 0.5 h). The other conditions were the same as those for slow drying films. The thickness of the films was in the range of 30−50 μm. After the films were dry, they were cut from the glass substrate and placed in the DSC pan (in the form of small pieces). Some NP-20 surfactant-containing samples were annealed for 1 h at 90 °C, prior to the DSC analysis.

Modulated Differential Scanning Calorimetry (MDSC) Measurements. MDSC measurements were carried out

using a Universal VI.6I TA DSC Instrument. The samples were run under N_2 with a 2 °C/min average heating and cooling rate. The modulations had an amplitude of ±1 °C every 60 s. For most samples three scans were performed: scan 1 (heating from −60 to +75 °C); scan 2 (cooling from +75 to −60 °C); scan 3 (reheating from −60 to +75 °C). The total measurement required about 5 h. T_g values were calculated automatically using the instrument software.

Fluorescence Decay Measurements. Fluorescence decay measurements were carried out as described previously,[6] and the areas under each decay curve were integrated and analyzed as described below. The donor, phenanthrene, was excited at 296 nm, and its emission was recorded at 350−360 nm. The characteristic (Förster) energy transfer distance for Phe and An is 23 Å.[30]

A useful measure of the extent of energy transfer (ET) in the system is the quantum efficiency of energy transfer Φ_{ET}, which we calculate from the donor fluorescence decay profiles $I_D(t')$ for films in the presence and absence of acceptor.

$$\Phi_{ET} = 1 - \frac{\int_0^\infty I_D(t')\,dt'}{\int_0^\infty I_D^{\,o}(t')\,dt'} = 1 - \frac{\text{Area}(t)}{\text{Area}([\text{An}] = 0)} \qquad (1)$$

The middle term represents the definition of the energy transfer efficiency in terms of the integrated intensity decay profiles, where the $I_D^{\,o}(t')$ is the donor decay profile in the absence of acceptor. For latex films containing phenanthrene as the donor, $I_D^{\,o}(t')$ is always exponential. Area(t) represents the integrated area under the fluorescence decay profile of a latex film sample annealed for a time t, and Area([An] = 0) refers to the area under the decay profile of a film containing only donor. To calculate these areas, nonexponential decay profiles are fitted to the stretched exponential in eq 2.

$$I_D(t') = B_1 \exp\left[-\frac{t'}{\tau_D} - P\left(\frac{t'}{\tau_D}\right)^{1/2}\right] + B_2 \exp\left(-\frac{t'}{\tau_D}\right) \qquad (2)$$

The fitting parameters B_1, B_2, and P in eq 2 obtained from each profile are useful for area integration, but their physical meaning is not important here. These integrated areas have dimensions of time, and define an average decay time $\langle\tau_D\rangle$ for the sample.

Results and Discussion

In the experiments described here, we prepare latex films in the presence and absence of NP-20 surfactant and in the presence of poly(ethylene glycol) oligomer (referred to as PEG or EO_x, where x describes the degree of polymerization of the oligomer). In the aqueous dispersion, the PBMA latices are spherical particles with a narrow size distribution, but upon drying at temperatures above the minimum film forming temperature (MFT), they deform and pack to yield transparent and mechanically continuous films. We refer to the Voronoi polyhedra formed by the particles as cells, and one of our main concerns in this paper is the influence of the surfactant and oligomer additives on the rate of polymer diffusion in the latex film across the intercellular boundary. We also show that at ambient temperature little mixing at the molecular level occurs between the additive and the latex polymer. This raises the other main concern in this paper, the location of the additive in the film, both in the newly formed films and in the films after annealing. Because we have shown previously that NP-20 acts as a plasticizer to promote polymer diffusion at elevated temperatures,[6] we also describe experiments which examine the binding of NP-20 to PBMA latex in water.

Energy Transfer Experiments. PBMA latex films containing only phenanthrene (Phe) as a fluorescent label exhibit an exponential fluorescence decay with a lifetime τ_D of 45 ns. Latex films prepared from a mixture of donor- and acceptor-labeled PBMA latex, with Phe as the donor and anthracene (An) as the acceptor, exhibit nonexponential donor fluorescence decay profiles because of direct nonradiative energy transfer (DET) from Phe to An in the films. In annealed films, polymer diffusion mixes the Phe- and An-labeled polymers from adjacent cells, bringing the two chromophores into proximity. In freshly prepared films cast just above the minimum film-forming temperature (MFT), little interdiffusion occurs, and the changes in the donor fluorescence decay profile $I_D(t')$ observed are due primarily to energy transfer across the interparticle boundary.

In newly formed films prepared near ambient temperature, values of Area(0) differ from that of Area([An] = 0). Since no polymer diffusion takes place at room temperature, we attribute this difference to transboundary energy transfer prior to the onset of polymer diffusion.[18] We have shown[19] that for a series of spherical high T_g donor-labeled particles, well-dispersed in a continuous acceptor-labeled matrix, the interfacial energy transfer efficiency increases with $1/d_p$, i.e., as the surface-to-volume ratio in the system, where d_p is the diameter of the latex. In a latex film prepared from a 1:1 mixture of donor- and acceptor-labeled particles, with a common level of acceptor label density, one expects a lower ET efficiency than in the case of the uniform surrounding acceptor-labeled matrix. For nascent films prepared from a 1:1 Phe/An mixtures of ca. 120 nm PBMA particles with the degree of labeling employed here, we often find $\langle\tau_D\rangle$ values of 42 ns, corresponding to an ET efficiency of 7%.

To calculate the "extent of mixing" f_m that occurs upon annealing the samples, we have to correct for transboundary ET:

$$f_m = \frac{\Phi_{ET}(t) - \Phi_{ET}(0)}{\Phi_{ET}(\infty) - \Phi_{ET}(0)} = \frac{\text{Area}(0) - \text{Area}(t)}{\text{Area}(0) - \text{Area}(\infty)} \qquad (3)$$

where $[\Phi_{ET}(t) - \Phi_{ET}(0)]$ represents the change in DET efficiency between the initially prepared film and that aged for time t. f_m is an important parameter for characterizing the extent of polymer diffusion in latex films. Strictly speaking, it represents the "quantum fraction" of mixing rather than the mass fraction of mixing f_s. For appropriate levels of acceptor labeling and for diffusion that satisfies Fick's laws, f_m and f_s are proportional up to f_m values up to ca. 0.7.[17,20]

To proceed more deeply into the analysis of the diffusion process, one needs to calculate diffusion coefficients characterizing the rate of polymer diffusion across the intercellular interface. This can be done at different levels of rigor and sophistication.[17,20] In our case, diffusion coefficients were calculated from f_m by fitting these data to a spherical Fickian diffusion model,[21] essentially assuming that $f_m = f_s$, where f_s is the fraction of mass that has diffused across the initial boundary. Simulations show that for the acceptor concentrations we employ that f_s is proportional to f_m for f_m values up to about 0.7. The details of this analysis, its convenience, and its shortcomings, have been discussed previously.[22] The values we obtain are apparent mean diffusion coefficients D_{app}, which rep-

resent an average over the polymers of broad molecular weight distribution in the sample, as well as the sample history. The importance of these numbers is that for samples with similar degrees of acceptor labeling, changes in D_{app}, compared at similar f_m values, correspond to changes in the true center-of-mass diffusion coefficients of the polymers.

Latex Films in the Presence of NP-20. In previous experiments in our laboratory,[6a] we observed that addition of NP-20 to dispersions of PBMA latex led to significant increases in the polymer diffusion rate for amounts of NP-20 ranging from 3 to 15 wt %. This influence was entirely consistent with the NP-20 acting as a traditional plasticizer for PBMA at the annealing temperature.

NP-20 Binding Isotherms. Isotherms were measured for the binding NP-20 surfactant to three samples of PBMA latex of different particle size. The experiments involved stirring the latex samples, cleaned of anionic surfactant remaining from the particle synthesis, with a known amount of NP-20. The solutions were centrifuged to sediment the particles, and the unbound NP-20 remaining in the supernate was measured by UV absorption spectroscopy. In each case, we observed Langmuir isotherms, with a common area per surfactant at saturation. Similar experiments on PBMA latex with other NP-EO_x surfactants indicated that the area per chain occupied by each surfactant at saturation was a sensitive function of the EO chain length, but not the particle size. For NP-20, this area is 115 Å^2, and for the 141 nm diameter particles examined here, saturation of the particle surface corresponds to about 6 wt % surfactant.

DET in Nascent Films. Because DET operates over such a short range (10−40 Å for Phe/An), the presence of unlabeled membrane material in the latex films will separate the donor- and acceptor-labeled polymer, and decrease the efficiency on interparticle energy transfer. Under these circumstances, the mean Phe decay time $\langle\tau_D\rangle$ will increase toward its unquenched value of 45 ns. The value of $\langle\tau_D\rangle$ is often known with great precision (better than by integrating the entire donor decay profile. The presence of interstitial material in newly formed latex film, which causes a significant decrease in the area of contact between adjacent cells in the film, will cause a measurable change in $\langle\tau_D\rangle$. On occasion, we observe this effect for anionic surfactants such as sodium dodecyl sulfate (SDS).[19] On the other hand, some coalescing aids promote interdiffusion during film formation, leading to higher values of $\Phi_{ET}(0)$ than expected for sharp intercellular interfaces.

Crack-free transparent films are formed in all NP-20-containing PBMA dispersions dried at 32 °C. In these freshly prepared films, we observe a measurable amount of DET. We plot our data in Figure 2, where we observe no change, within experimental error, in the magnitude of Area(0) over a broad range of NP-20 concentrations ranging from 0 to 15 wt %. From our binding isotherm measurements, we know that 6.5 wt % surfactant corresponds to monolayer coverage of the PBMA particles. The value of $\langle\tau_D\rangle = 42$ ns, compared to $\tau_D = 45$ ns in the acceptor-free film indicates that there is no extensive interconnected surfactant membrane structure in these films. There are two possible explanations for this result. The first, which had a strong appeal for us, was that the surfactant was able to diffuse into the latex polymer even at 32 °C. We will see below that this explanation is incorrect. Alternatively, expulsion of the surfactant from the interstitial spaces would lead to surfactant domains within the film. Under these circumstances, the surfactant occlusions might have a negligible effect on the cell surface area probed by the DET experiments in the newly formed films.

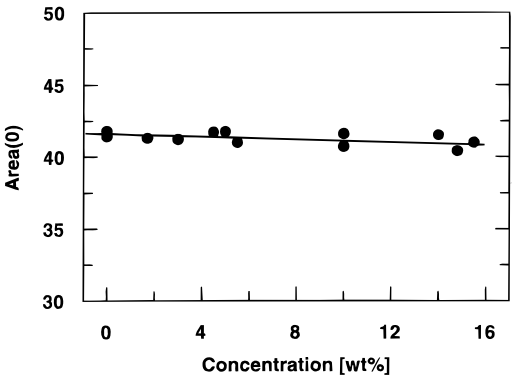

Figure 2. Plots of Area(0) values (obtained from integration of the normalized Phe fluorescence decay profiles) vs concentration of NP-20 surfactant molecules.

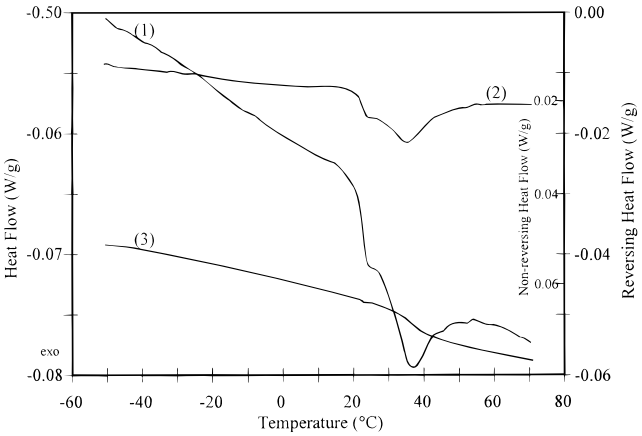

Figure 3. Plots of heat flow (1), nonreversing heat flow (2), and reversing heat flow (3) vs temperature for pure PBMA. The reversing heat flow shows a glass transition at 34 °C. The peak in the scan of nonreversing heat flow is due to enthalpy relaxation reflecting prior sample history.

Differential Scanning Calorimetry Experiments. MDSC is a recent variation of differential scanning calorimetry in which a sinusoidal temperature perturbation is applied.[23,24] The advantages of MDSC include the ability to separate overlapping phenomena, as well as to improve measurement resolution and sensitivity.[23] Various applications have been reported. These include the separation of the recrystallization peak from the glass transition,[25] separation of physical aging annealing peaks from the glass transition,[25,26] measurements of absolute heat capacity,[27,28] and the measurements of thermal conductivity.[29] An example of the total, reversing and nonreversing heat flow for pure PBMA is shown in Figure 3. The term "reversing" refers to the part of the process that is reversible on the time scale of the oscillations. From reversing heat flow we see very clearly the glass transition $T_g = 34$ °C. From the nonreversing heat flow we observe the peak that comes only from the sample's preparation history. NP-20 is a crystalline material, and the formation of surfactant occlusions in the polymer films should lead to a melting transition measurable by DSC. Since the melting

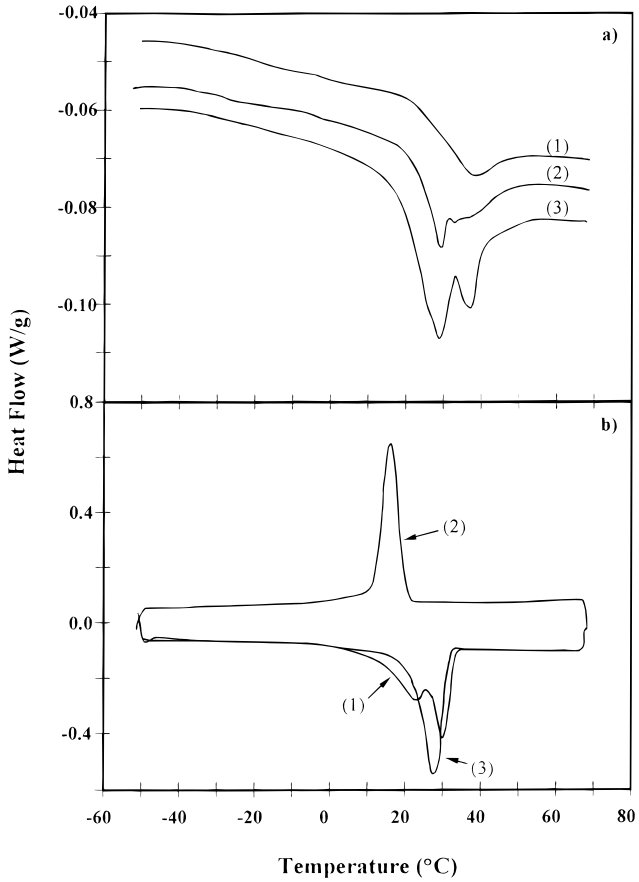

Figure 4. (a) MDSC first scans (heating) for pure PBMA (1), PBMA + 5 wt % NP-20 (2), and 10 wt % NP-20 (3). (b) MDSC scans (first heating (1), second cooling (2), and third reheating (3) for pure NP-20 surfactant.

temperature occurs in the same temperature range as the glass transition of PBMA, we turned to modulated DSC, which allows us to separate the glass transition from other interfering transitions in the sample.

In Figure 4a we show typical MDSC first heating scans for pure PBMA, and for PBMA latex films containing 5 wt % and 10 wt % of NP-20 surfactant. Figure 4b shows the MDSC first heating scan (melting), second cooling scan (crystallization), and third scan (melting) for the pure NP-20 surfactant. Over the same range of temperatures (between 20 and 40 °C), one can observe three overlapping events: the glass transition of the polymer, the exotherm peak from enthalpy relaxation in the sample, and the melting transition for the surfactant. The glass transition is a reversible transition superimposed upon the melting transition and the nonreversing part of the heat flow due to sample preparation history. To separate these events, we consider the cooling scan (Figure 4b), where the crystallization exotherm for pure NP-20 is detected in the nonreversing component of the total heat flow. We note that the crystallization exotherm has an area similar to that of the melting endotherm seen on the reheating scan and is shifted somewhat to lower temperature. The temperature shift depends on the relative temperature ramp (cooling, heating rate) compared to the time required for crystallization to take place.

We see remarkably different behavior in MDSC traces of PBMA + NP-20 mixtures. For example, when we add 5 wt % or more of NP-20 to the PBMA, a crystallization exotherm can be observed in the nonreversing component of the cooling scan. It appears at very low temperatures (e.g., −40 °C) and is smaller in magnitude than the melting exotherm, observed in either the first heating scan or the reheating scan. An example is given in Figure 5. The shift in the position of the crystallization exotherm compared to the melting endotherm is at first surprising. We explain this behavior as follows. In the newly formed film, most of the NP-20 is present in its crystalline form. As the sample is heated, the substance melts. We know that at sufficiently high temperature (90 °C), the NP-20 molecules diffuse into the PBMA polymer phase and mix molecularly with the polymer. As the sample is cooled, demixing occurs. This takes time. The exact position of the crystallization endotherm, and its breadth, depend on the rate of demixing compared to the rate of cooling of the sample. In this sense, the crystallization endotherm differs significantly from that observed for the pure surfactant, which crystallizes more rapidly on cooling.

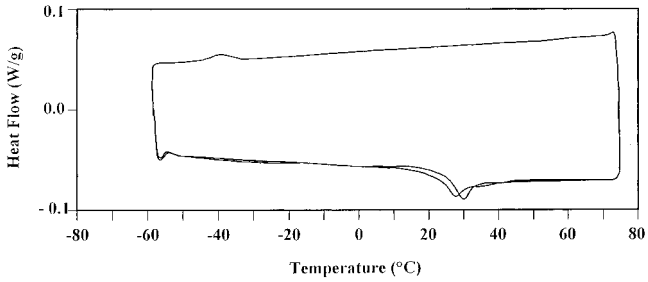

Figure 5. Plot of total heat flow vs temperature (three scans) for PBMA + 5 wt % NP-20. We identify the small broad exotherm at −40 °C in the cooling scan with the crystallization of NP-20 after it demixes from the polymer.

Table 3. Summary of T_g values for PBMA and PBMA + 2 wt% NP-20 blends

	T_g (°C)[a]	
scan	PBMA	PBMA + 2 wt % NP-20
first, heating	36.3	34.8
second, cooling	34.1	30.5
third, heating	33.6	30.4

[a] The estimated error in all T_g measurements reported here is ±0.5 °C.

We are particularly interested in the influence of NP-20 on the glass transition temperature of the PBMA matrix. Films containing only 2 wt % surfactant exhibit no melting or recrystallization transitions for the surfactant, on either heating or cooling. There is, however, a measurable decrease in the T_g of the polymer, which can be observed in all three scans. In Table 3 we report values of T_g for PBMA and for PBMA containing 2 wt % NP-20. For PBMA itself, we find a small decrease in the calculated T_g values on successive scans, a sample history effect. There are similar effects of sample history on the sample containing 2 wt % NP-20, with lower T_g values in the presence of this small amount of surfactant. We note that the NP-20 has a larger effect on lowering T_g in the second and third scans than in the first scan, where the change in T_g is only 1.6 °C. For the second and third DSC scans the change has increased to 3.6 °C. While this difference is not large, and the estimated precision in T_g is 0.5°, these observations are consistent with only partial mixing of the surfactant and polymer during the film formation. More extensive mixing and a more uniform distribution of the surfactant in the polymer phase takes place following the first heating scan. During the first heating scan

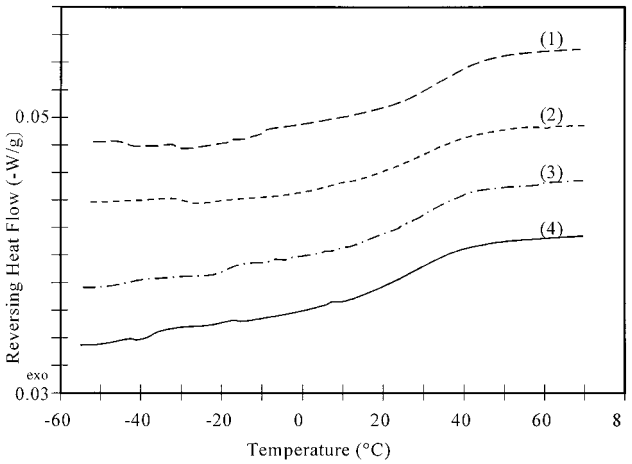

Figure 6. Plots of reversing heat flow (W/g) for the cooling scan vs temperature for PBMA (1), PBMA + 2 wt % NP-20 (2), PBMA + 5 wt % NP-20 (3), and PBMA + 10 wt % NP-20 (4).

Table 4. Summary of T_m Values[a] for NP-20 and T_g Values[b] for PBMA (in °C) for NP-20 and for Mixtures of PBMA with Various Amounts of NP-20

material	NP-20	PBMA	PBMA + NP-20 2 wt %	PBMA + NP-20 5 wt %	PBMA + NP-20 10 wt %
T (°C)	16[a]	34 ± 0.5[b]	30.5 ± 0.5[b]	29 ± 0.5[b]	29 ± 0.5[b]

[a] Crystallization peak obtained on the cooling scan. [b] Glass transition temperatures obtained on the cooling scan.

and subsequent cooling scan, the sample spends about 40 min at temperatures between 50 and 75 °C. In our view, it is during this time that the surfactant diffuses into the PBMA phase.

To study the influence of larger amounts of NP-20 on the polymer T_g, we obtain information from the reversing component of the cooling scan. In the first heating scan and in the reheating scan, the glass transition is masked by the melting of the NP-20. In Figure 6 we show the reversing heat flow for the cooling scan for a sample of PBMA itself, and for PBMA samples containing 2, 5, and 10 wt % NP-20. These latex films were all prepared under slow drying conditions. The results are summarized in Table 4. We find that 2 wt % NP-20 causes a 4 °C decrease in the T_g of the polymer, whereas further addition of NP-20 leads to only a small additional decrease (1 °C) in T_g. These results suggest that at temperatures near room temperature, the system has reached the limits of miscibility at a surfactant content between 2 wt % and 5 wt %. Even this conclusion is subject to sample history effects. When the sample containing 5 wt % NP-20 is annealed for 1 h at 90 °C, the polymer exhibits a $T_g = 27.3$ °C ($\Delta T_g =$ 7 °C) on the subsequent cooling scan. These results establish that for NP-20 in PBMA latex films near room temperature, some of the surfactant dissolves in the polymer and some is present in the form of aggregates or occlusions sufficiently large to exhibit both melting and crystallization transitions.

Mixtures of PBMA with EO_{10} and EO_{20} Examined by MDSC. The results for PBMA latex films prepared in the presence of the PEG oligomer EO_{20} are presented in Table 5. For all of the samples, containing 3.8 wt %, 5 wt %, and 10 wt % EO_{20}, the measured T_g's are identical to that of the PBMA polymer itself. From this result, we deduce that EO_{20} and PBMA are essentially immiscible over the temperature range of our measurements. This conclusion is confirmed by polymer diffusion studies described below, where we have observed that the presence of EO_{20} in PBMA latex films retards PBMA diffusion in the film. We suspect that EO_{20} may form a hydrophilic membrane in the film that acts as a barrier to interparticle polymer diffusion.

Table 5. Summary of T_g and T_m Values (°C) for EO_{20} and (PBMA + EO_{20})

		PBMA + EO_{20} (T_g)		
scan	EO_{20}	3.9 wt %	5.1 wt %	9.4 wt %
heating[a]	32.6[b]			
cooling	24.9[c]	32.9	32.2	32.0

[a] The PBMA T_g is obscured by contributions of EO_{20} melting to the reversing heat flow. [b] Melting peak. [c] Crystallization peak.

Table 6. Summary of T_g and T_m Values (°C) for EO_{10} and (PBMA + EO_{10})

		PBMA + EO_{10} (T_g)		
scan	EO_{10}	1.7 wt %	3.6 wt %	5.1 wt %
first, heating	0.8[a]	34.0	34.5	34.0
second, cooling		29.5	30.8	29.5
third, heating		34.5	33.8	31.7

[a] Melting peak.

The results for films prepared from PBMA latex + EO_{10} are presented in Table 6. The melting transition of the EO_{10} ($T_m = 0.8$ °C) is well separated from the glass transition of PBMA, so that we were able to obtain PBMA T_g values from all three MDSC scans. Here a small but significant decrease of T_g (about 3.5 °C) is observed during the cooling scan (i.e., after the sample has been heated); but no change in T_g can be detected on either the first or second heating scan. Diffusion experiments show that EO_{10} causes a slight increase in the diffusion rate of polymer for annealed samples. These results suggest that there is some miscibility between the two components at high temperature, but they phase separate at low temperature.

Effect of EO_x on Interdiffusion in PBMA Latex Films. Because of the limited miscibility observed by MDSC for the EO_x oligomers with the high molecular weight PBMA sample, we examined the influence of these oligomers on both high and low molecular weight PBMA latex films, and we also carried out experiments at two different temperatures. The results at an annealing temperature of 76 °C for films prepared from the high molecular weight PBMA sample in the absence and presence of 5 wt % PEG are shown in Figure 7. In Figure 7a,b we plot the time dependence of the extent of mixing f_m and the calculated apparent diffusion coefficients D_{app}, respectively; and in Figure 7c we plot D_{app} as a function of f_m.

In previous publications, we have reported D_{app} values only as a function of f_m, since it is only at common values of f_m that one can make quantitative comparisons of diffusion rates between different samples. Linear plots of D_{app} vs time, however, emphasize that a significant amount of interdiffusion occurs at early times, and here, for the sample without added PEG, one observes a very rapid drop in D_{app} values at early stages of polymer interdiffusion. This mixing involves the lowest molecular weight components of the latex polymers. The presence of a labeled low molecular weight tail in the PBMA molecular weight distribution can be seen in gel permeation chromatography experiments and is a con-

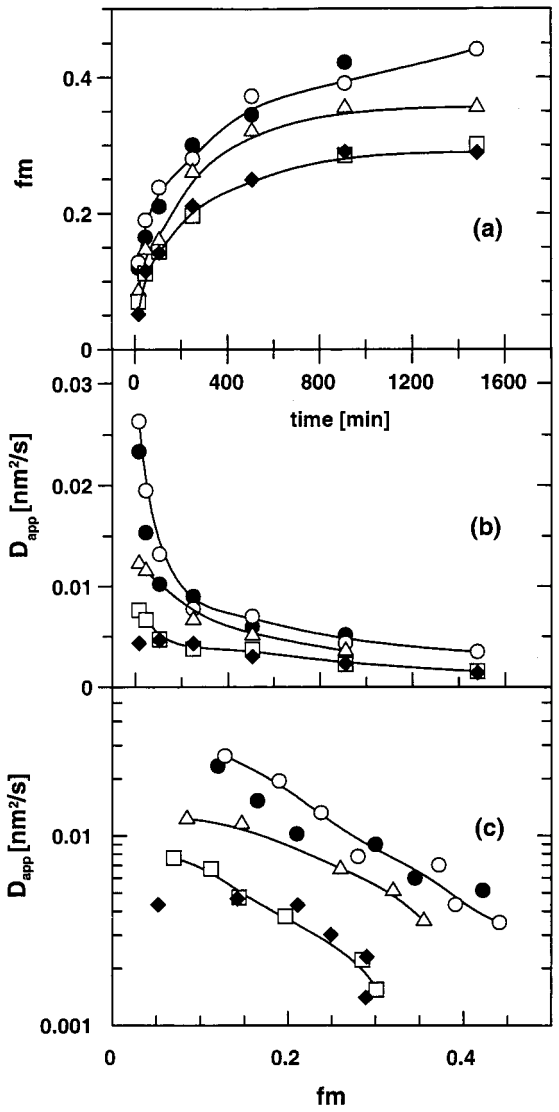

Figure 7. Dependence of extent of diffusion f_m (a) and apparent diffusion coefficient D_{app} (b) on annealing time (diffusion time). (c) Dependence of diffusion coefficient on extent of mixing for pure PBMA film (●) and films with the presence of 5 wt % PEG of different molecular weight (○) EO_{10}, (△) EO_{20}, (□) EO_{68}, (◆) EO_{100}). Annealing temperature: 76 °C

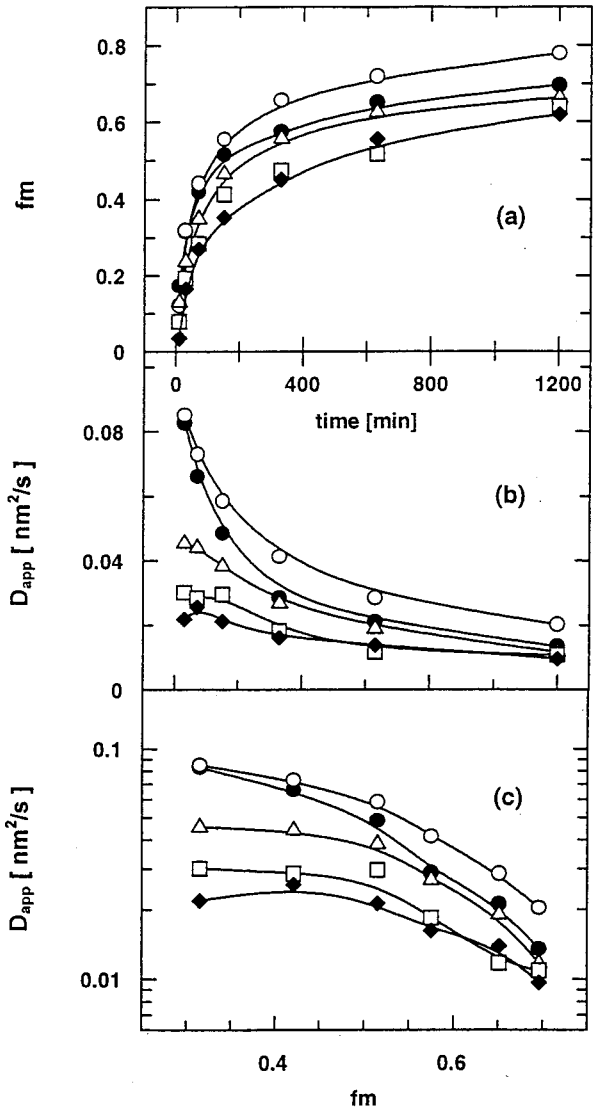

Figure 8. Dependence of extent of diffusion f_m (a) and apparent diffusion coefficient D_{app} (b) on annealing time (diffusion time). (c) Dependence of diffusion coefficient on extent of mixing for pure PBMA film (●) and films with the presence of 5 wt % PEG of different molecular weight (○) EO_{10}, (△) EO_{20}, (□) EO_{68}, (◆) EO_{100}). Annealing temperature: 90 °C.

sequence of our preparing the latex under monomer-starved conditions. The broad molecular weight distribution of the sample also contributes to the continuing decrease in D_{app} values at later times, as seen in Figure 7b,c. Once the most mobile components of the polymer have intermixed, the increase in ET measured in the experiment is due to interdiffusion by somewhat less mobile polymer, and near the end of the experiment, as f_m approaches unity, the slowest diffusing polymer contributes to the growth in ET. We remind the reader that the ET experiment is sensitive to diffusion on the length scale of the particle diameter. Diffusion can occur over much longer distances, but the ET experiment loses sensitivity once all the Phe-PBMA has mixed with An-PBMA.

From the data in Figure 7, it is clear that at 76 °C, the presence of PEG at 5 wt % retards the rate of polymer diffusion, and that this effect is more pronounced with higher molecular weight oligomer. For EO_{10}, the effect is too small to be observed, whereas longer chain derivatives (EO_{20}, EO_{68}, EO_{100}) have an increasingly larger effect on the rate of mixing. In Figure 7b we see that there is a particularly large effect on the interdiffusion rate at early times in the diffusion process. These results are consistent with the formation of a polar hydrophilic membrane by the PEG in the PBMA latex film, which could serve as a barrier to polymer diffusion across the intercellular boundaries. Based upon arguments described above, we would expect that if the PEG oligomers acted in this way, we would observe an increase in Area(0) from 42 ns with the addition of increasing amounts of PEG. To our surprise we find no change in the efficiency of DET in newly formed films with an added PEG component.

A second set of experiments carried out at 90 °C gave similar results. The data are presented in Figure 8. At 90 °C, the presence of 5 wt % EO_{20}, EO_{68}, or EO_{100} suppresses the polymer interdiffusion rate. Here we find that EO_{10} actually increases the diffusion rate to a small extent. These results are consistent with limited miscibility of the short PEG oligomer with PBMA at elevated temperatures.

Three experiments were carried out with the low molecular weight PBMA sample (M_w = 35 000). Be-

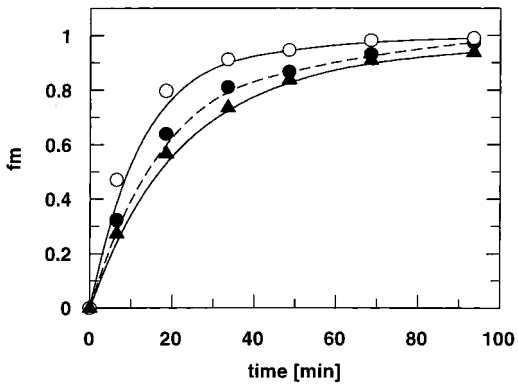

Figure 9. Dependence of extent of diffusion (f_m) on annealing time (diffusion time) for pure low Mw PBMA film (●) and films with the presence of 5 wt % PEG of different molecular weight (○) EO_{10}, (▲) EO_{45}). Annealing temperature: 60 °C.

cause of the much faster polymer diffusion rate for this sample, the films were annealed simultaneously at 60 °C. In Figure 9 we plot f_m vs time for these samples. Here we see that EO_{10} acts as a plasticizer to promote the polymer mixing rate whereas 5 wt % EO_{45} causes a small retardation. The shorter the EO oligomer and the shorter the PBMA chains, the greater their miscibility, a situation typical of polymers of borderline immiscibility.

Conclusions

The nonionic surfactant NP-20 has only limited miscibility with PBMA at room temperature. Miscibility at room temperature is detected as a lowering of the polymer T_g, and the limit of miscibility inferred from these measurements is slightly more than 2 wt %. As the samples are heated, the components become more miscible, and at 90 °C the surfactant is fully miscible with the polymer in amounts up to at least 15 wt %, as was shown in polymer diffusion experiments by Kawaguchi et al.[6] Thus these components are characterized by an upper critical solution temperature.

We are interested in the location of the NP-20 in the latex film as a function of sample history. The smaller change in polymer T_g on the first heating scan (ΔT_g = 1.5 °C) for the 2 wt % sample, compared to the change that occurs following sample annealing (ΔT_g = 3 °C), suggests that there is limited diffusion of the surfactant into the surface regions of the latex during film formation at 32 °C. More extensive mixing occurs once the sample is heated. Attempts to repeat these measurements in the presence of higher concentrations of NP-20 are frustrated by poor data when the melting endotherm occurs in the same temperature range (e.g., on heating) as the glass transition. Full miscibility occurs when the sample is heated to 90 °C, and the crystallization endotherm observed on the cooling scan is due to surfactant which demixes and then crystallizes in the sample. The implication of this result is that in the polymer interdiffusion experiments of Kawaguchi,[6] the components mixed rapidly when the samples were heated to 90 °C. Each time he removed samples from the oven and cooled them to room temperature for the fluorescence decay measurements, the NP-20 must have demixed, but these phase-separated domains caused no interference with the fluorescence decay measurements of polymer interdiffusion. A drawing depicting our view of this process is presented in Figure 10.

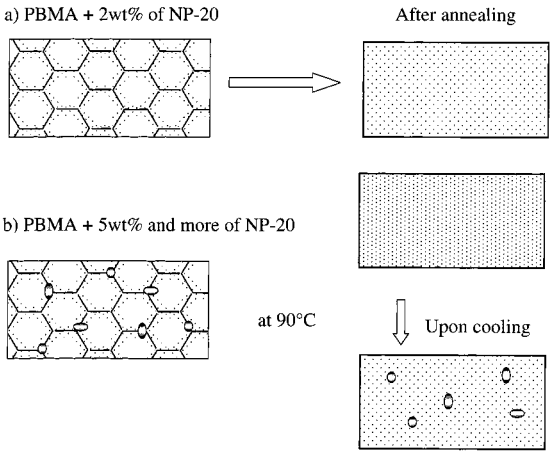

Figure 10. Model of NP-20 surfactant distribution in PBMA latex films with varying surfactant content. (a) For PBMA films with 2 wt % or less of NP-20 surfactant. Before annealing, the surfactant is distributed only in the top surface of the polymer. After annealing, the surfactant is uniformly distributed in the film. (b) For PBMA films with 5+ wt % NP-20 surfactant. Before annealing, the surfactant is distributed only in the top surface of the polymer. During annealing at 90 °C, the surfactant diffuses uniformly into the polymer phase. Upon cooling, part of the surfactant remains in the polymer phase, but the rest of the NP-20 phase separates and forms local domains in the film.

By MDSC, neither EO_{10} nor EO_{20} show any evidence for miscibility with PBMA near room temperature, either in freshly prepared or annealed samples. ET measurements of polymer interdiffusion show that all EO oligomers of 20 or more EO units act to retard polymer diffusion. The source of this retardation is not yet clear. We suspect that the PEG chains become trapped at the particle surface and form a polar membrane, which acts as a barrier to polymer diffusion. We do not, however, observe an increase in Area(0) in the freshly prepared films. If the PEG oligomers served to separate the individual Phe-PBMA and An-PBMA cells and decrease the trans-boundary ET, then Area(0) would increase above 42 ns. A possible explanation for both effects is that the presence of the PEG promotes some mixing of polar components at the latex particle surface, and this mixture serves as the membrane barrier to retard further polymer diffusion.

EO_{10} is sufficiently small that it has some miscibility with PBMA at elevated temperatures. It promotes the diffusion rate of high molecular weight PBMA (M_w = 450 000) at 90 °C (but not at 76 °C) and has an even larger effect on the diffusion of low molecular weight PBMA (M_w = 35 000) at 60 °C.

Acknowledgment. The authors thank ICI, ICI Canada, and NSERC Canada for their support of this research.

References and Notes

(1) Tanaka, T.; Fujimoto, T.; Sibayama, K. *J. Appl. Polym. Sci.* **1979**, *23*, 1131.
(2) Haq, Z.; Thompson, L. *Colloid Polym. Sci.* **1982**, *260*, 212.
(3) Eckersley, S. T.; Rudin, A. *J. Appl. Polym. Sci.* **1993**, *48*, 1369.
(4) Snuparek, J.; Hanus, A. J., Jr.; Hajkova, B. *J. Appl. Polym. Sci.* **1983**, *28*, 1421.
(5) Roulstone, B. J.; Wilkinson, M. C.; Hearn, J. *Polym. Int.* **1992**, *27*, 43.
(6) Kawaguchi, S.; Odrobina, E.; Winnik, M. A. *Macromol. Rapid Commun.* **1995**, *16*, 861. (b) Fujita, H. *Fortschr. Hochpolym.-Forsch.* **1961**, *3*, 1.

(7) Bradford, E. B.; Vanderhoff, J. W. *J. Macromol. Chem*. **1966**, *1*, 335.
(8) Bradford, E. B.; Vanderhoff, J. W. *J. Macromol Sci., Phys*. **1972**, *B6*, 671.
(9) Chevalier, Y.; Pichot, C.; Grailat, C.; Joanicot, M.; Wong, K.; Maquet, J.; Lindner, P.; Cabane, B. *Colloid Polym. Sci*. **1992**, *270* (8), 806.
(10) Voyutskii, S. S. *J. Polym. Sci*. **1958**, *32*, 528.
(11) Wang, Y.; Kats, A.; Juhué, D.; Winnik, M. A.; Shivers, R. R.; Dinsdale, C. J. *Langmuir* **1992**, *8*, 1435.
(12) Winnik, M. A.; Feng, J. *J. Coat. Technol*. **1996**, *68* (852), 39.
(13) Juhué, D.; Lang, J. *Langmuir* **1993**, *9*, 792.
(14) Joanicot, M.; Wong, K.; Maquet, J.; Chevalier, Y.; Pichot, C.; Grailat, C.; Lindner, P.; Rios, L.; Cabane, B. *Prog. Colloid Polym. Sci*. **1990**, *81*, 175.
(15) Feng, J. Ph.D. Thesis, University of Toronto, 1996.
(16) Wang, Y.; Winnik, M. A. *J. Phys. Chem*. **1993**, *97*, 2507. Kim, H.-B.; Winnik, M. A. *Macromolecules* **1994**, *27*, 1779.
(17) Dhinojwala, A.; Torkelson, J. M. *Macromolecules* **1994**, *27*, 4817. Liu, Y. S.; Feng, J.; Winnik, M. A. *J. Chem. Phys*. **1994**, *101*, 9096. Kim, H.-B.; Winnik, M. A. *Macromolecules* **1995**, *28*, 2033.
(18) Feng, J.; Pham, H.; Stoeva, V.; Winnik, M. A. *J. Polym. Sci., Polym. Phys*. **1998**, *36* (7), 1129.
(19) Feng, J.; Winnik, M. A.; Siemiarczuk, A. *J. Polym. Sci., Polym. Phys*. **1998**, *36* (7), 1115.
(20) Yekta, A.; Duhamel, J.; Winnik, M. A. *Chem. Phys. Lett*. **1995**, *235*, 119. Farinha, J.; Martinho, J. M. G.; Yekta, A.; Winnik, M. A. *Macromolecules* **1994**, *27*, 1994.
(21) Crank, J. *The Mathematics of Diffusion*; Clarendon: Oxford, U.K., 1975.
(22) Kim, H.-B.; Winnik, M. A. *Macromolecules* **1994**, *27*, 1007.
(23) Reading, M. *Trends Polym. Sci*. **1993**, *8*, 248.
(24) Gill, P. S.; Sanerbrunn, S. R.; Reading, M. *J. Therm. Anal*. **1993**, *40*, 931.
(25) Reading, M.; Elliott, D.; Hill, V. L. *J. Therm. Anal*. **1993**, *40*, 949.
(26) Hourston, D. J.; Song, M.; Hammiche, A.; Pollock, H. M.; Reading, M. *Polymer* **1996**, *37* (2), 243.
(27) Boller, A.; Jin, Y.; Wunderlich, B. *J. Therm. Anal*. **1994**, *42*, 307.
(28) Varma-Nair, M.; Wunderlich, B. *J. Therm. Anal*. **1996**, *46*, 879.
(29) Marcus, S. M.; Blaine, R. L. *Thermochim. Acta* **1994**, *243*, 231.
(30) Wang, Y.; Zhao, Ch.-L.; Winnik, *M. A. J. Phys. Chem*. **1991**, *95*, 2143.

MA971870C